Inflammation, Vol. 42, No. 5, October 2019 (© 2019)
DOI: 10.1007/s10753-019-01052-8

ORIGINAL ARTICLE

Fraxin Alleviates LPS-Induced ARDS by Downregulating Inflammatory Responses and Oxidative Damages and Reducing Pulmonary Vascular Permeability

Xiaohong Ma,[1,2] Xiangyong Liu,[1,4] Jiali Feng,[1,2] Dong Zhang,[1,2] Lina Huang,[1] Dongxiao Li,[1,2] Liang Yin,[3] Lan Li,[1] and Xiao-Zhi Wang[2]

Abstract— Acute respiratory distress syndrome (ARDS) is a severe acute disease that threatens human health, and few drugs that can effectively treat this disease are available. Fraxin, one of the main active ingredients of Cortex Fraxini, a Chinese herbal medicine, has presented various pharmacological and biological activities. However, the effects of fraxin on ARDS have yet to be reported. In the present study, the protective effect of fraxin in lipopolysaccharide (LPS)-induced ARDS in a mouse model was analyzed. Results from the hematoxylin and eosin staining showed that fraxin might alleviate pathological changes in the lung tissues of mice with ARDS. ELISA and Western blot results revealed that fraxin might inhibit the production of inflammatory factors, namely, IL-6, TNF-α, and IL-1β, and the activation of NF-κB and MAPK signaling pathways in the lungs. Thus, the inflammatory responses were reduced. Fraxin might inhibit the increase in reactive oxygen species (ROS) and malondialdehyde (MDA), a product of lipid peroxidation in lung tissues. Fraxin might increase the superoxide dismutase (SOD) activity to avoid oxidative damage. Vascular permeability was also assessed through Evans blue dye tissue extravasation and fluorescein isothiocyanate–labeled albumin (FITC-albumin) leakage. Fraxin might inhibit the increase in pulmonary vascular permeability and relieve pulmonary edema. Fraxin was also related to the inhibition of the increase in matrix metalloproteinase-9, which is a glycocalyx-degrading enzyme, and the relief of damages to the endothelial glycocalyx. Thus, fraxin elicited

Xiaohong Ma, Xiangyong Liu and Jiali Feng contributed equally to this work.

[1] Department of Cell Biology, Binzhou Medical University, Yantai, 264003, Shandong Province, China
[2] Department of Respirator Medicine and Intensive Care Unit, Affiliated Hospital of Binzhou Medical University, Binzhou, 256603, Shandong Province, China
[3] Department of Immunology, the School of Basic Medical Sciences, Shandong University, Jinan, 250012, Shandong Province, China
[4] To whom correspondence should be addressed at Department of Cell Biology, Binzhou Medical University, Yantai, 264003, Shandong Province, China. E-mail: liuxiangyong81@gmail.com

protective effects on mice with LPS-induced ARDS and might be used as a drug to cure ARDS induced by Gram-negative bacterial infection.

KEY WORDS: fraxin; lipopolysaccharide; ARDS; inflammatory responses; oxidative damages; pulmonary vascular permeability.

INTRODUCTION

Acute respiratory distress syndrome (ARDS), which is characterized by complex etiopathogenesis (*e.g.*, severe infection, shock, trauma, and burns), quick onset, rapid progress, and high mortality, seriously threatens the lives of patients [1, 2]. Few drugs that can effectively cure ARDS are available. Thus, intensive studies on the screening of drugs for ARDS treatment and the corresponding pharmacological mechanisms are important to prevent and control ARDS [3].

ARDS has a complex pathogenesis that involves (1) severe inflammatory responses, including the overactivation of signaling pathways, such as NF-κB and mitogen-activated protein kinase (MAPK), which regulate the inflammatory responses and excessive generation of inflammatory factors, such as TNF-α and IL-6 [4, 5]; (2) excessive oxidative stress, which may result in the massive accumulation of reactive oxygen species (ROS) and oxidative damages to lung tissues [6, 7]; and (3) damages to the integrity of the endothelial glycocalyx, which may trigger an increase in the permeability of pulmonary capillary and lead to pulmonary edema [8, 9].

Fraxin is a coumarin compound, and it is the main ingredient of Cortex Fraxini, a Chinese herbal medicine [10]. Fraxin exhibits various pharmacological actions and biological activities [11, 12], such as anti-inflammation [13], antioxidation [14, 15], and hepatotoxicity reduction [12]. However, the effects of fraxin on ARDS have yet to be reported.

In the present study, the effects and possible mechanisms of fraxin on a mouse model of bacterial endotoxin lipopolysaccharide (LPS)-induced ARDS were investigated, adding a new theoretical basis for the development of drugs to treat ARDS.

MATERIALS AND METHODS

Laboratory Animals

C57BL/6 male mice weighing 18–20 g and aged 8–10 weeks old were provided by Jinan Pengyue Laboratory Animal Breeding Co., Ltd. They were placed at 24 ± 1 °C with a relative humidity of 40–80% and a 12-h:12-h light/dark cycle. All of the mice well adapted to the environment for 2–3 days before all of the subsequent experiments were conducted. All of the animal experiments were performed in accordance with the guide for the Care and Use of Laboratory Animals established by the US National Institutes of Health.

Drugs and Reagents

Fraxin (purity of ≥ 98%, Chengdu Must Biotechnology, China), LPS (from *Escherichia coli* 055:B5, L2880), Evans blue dye (EBD, E2129), 2′,7′-dichlorofluorescein diacetate (DCFH-DA, D6883), 4′,6-diamidino-2-phenylindole dihydrochloride (DAPI, D8417), and albumin-fluorescein isothiocyanate conjugate (FITC-albumin, A9771) were purchased from Sigma-Aldrich. Commercial determination kits for malondialdehyde (S0131), superoxide dismutase (SOD) (S0101), TNF-α (PT512), IL-6 (PI326), and IL-1β (PI301) were acquired from Beyotime Biotechnology (China). A murine CD138 (syndecan-1 [SDC-1]) ELISA kit (860.090.096) was obtained from Diaclone (France). Rabbit monoclonal antibody to JNK (ab112501), ERK (ab184699), p38 (ab170099), p65 (ab32536), IκBα (ab32518), p-ERK (ab201015), p-JNK (ab4821), p-p38 (ab47363), p-IκBα (ab133462), LaminB1 (ab133741), MMP-9 (ab38898), SDC-1 (ab128936), and FITC (ab25539) were bought from Abcam (USA). Peroxidase-conjugated AffiniPure goat anti-rabbit IgG (H+L) (ZB-2301), goat serum blocking solution (ZLI-9022), and rabbit serum blocking solution (ZLI-9026) were procured from Zhongshan Golden Bridge Biotechnology (China). Goat anti-rabbit IgG/Alexa Fluor 594 (bs-0295G-AF59), β-actin (bs-0061R), and rabbit anti-goat IgG/PE (bs-0294R-PE) were purchased from Bioss (China). Lastly, thrombomodulin/BDCA-3 (AF3894) was obtained from R&D Systems (USA).

Modeling and Grouping of Mice with ARDS

All of the mice were randomly divided into five groups: control, LPS group, and LPS + fraxin groups at 10, 20, or 40 mg/kg fraxin, and six mice were used in each group. The fraxin dosage used in this study was based on pre-experimental results and previous report [13]. The

treated groups were intragastrically administered with fraxin based on their body weight (10, 20, or 40 mg/kg), whereas the control and LPS groups were treated with the same volume of normal saline once a day. After the drugs were intragastrically administered for 7 consecutive days, the LPS + fraxin groups and the LPS groups were intraperitoneally injected with LPS (20 mg/kg) to induce the ARDS mouse model. The administration time of fraxin for 7 days in the study was based on previous report [13]. The control group was administered with the same volume of normal saline. After 6 h, the mice were intraperitoneally injected with 4% chloral hydrate, and the lung tissues were sampled through thoracotomy.

Histopathological Examination of the Mouse Lung Tissues

The mouse lung tissues were fixed with 4% paraformaldehyde for 24 h, dehydrated for 12 h, and embedded in paraffin. Then, the samples were prepared into 4-μm-thick slices. The slides were stained with hematoxylin and eosin (H&E) and examined pathologically under an optical microscope. Lung injury was scored by a blinded observer using a five-point scale in accordance with the combined assessments of the alveolar congestion, hemorrhage, infiltration, or aggregation of neutrophils in the airspace or the vessel wall and the thickness of alveolar wall/hyaline membrane formation: 0, minimum damage; l, mild damage; 2, moderate damage; 3, severe damage; and 4, maximum damage [16–18].

Determination of the Wet/Dry Ratio of the Mouse Lung Tissues

The whole lungs were extracted, and all of the bloodstains were wiped off from the lung surface by using an absorbent filter paper. The wet weight of the lungs was measured. After the surface was dried for 48 h in an oven at a constant temperature of 60 °C, the dry weight was measured. Then, the wet/dry (W/D) ratio was calculated.

Determination of the Contents of Pro-Inflammatory Cytokines (IL-6, TNF-α, and IL-1β) in the Bronchoalveolar Lavage Fluid of the Mice

Catheters were inserted in the trachea of the mice through tracheotomy under anesthesia. Bronchoalveolar lavage fluid (BALF) was processed with 0.5 mL of phosphate buffer solution (PBS) once, and this process was repeated thrice. The recycled BALF was centrifuged at 3000 rpm for 20 min at 4 °C. The supernatant was then recovered [19]. In accordance with the manufacturer's instructions of commercial ELISA kits of IL-6, TNF-α, IL-1β (Beyotime Biotechnology, China), the procedures were performed, and the IL-6, TNF-α, IL-1β contents in the BALF were determined.

Determination of the Malondialdehyde Content and the Superoxide Dismutase Activity in the Mouse Lung Tissues

Fresh lung tissues were weighed (60–80 mg), and the right amount of PBS was added. The lung tissue samples were fully homogenized and allowed to stand for 30 min. Then, the homogenized lung tissues were centrifuged at 3000 rpm at 4 °C for 20 min, and the supernatant was collected. The malondialdehyde (MDA) content and the SOD activity in the supernatants were determined in accordance with the instructions of MDA and SOD kits (Beyotime Biotechnology, China). The optical densities of the MDA and SOD supernatants were measured at 532 and 450 nm on a microplate reader, respectively. A relative standard curve was utilized to quantitate the MDA contents and the SOD activities in the mouse lung tissues individually. The MDA contents and the SOD activities were expressed as nanomole per milligram of protein (nmol/mg protein) and units per milligram of protein (U/mg protein), respectively.

Determination of the ROS Content in the Mouse Lung Tissues

Nonfluorescent DCFH-DA that enters cells through the cell membrane can be oxidized into fluorescent DCF by intracellular ROS, and its fluorescence intensity is proportional to ROS levels [20]. The ROS content was determined as follows. After the fluorescent dye DCFH-DA (1 mmol/L) was mixed with the supernatant of the homogenized lung tissues, the optical density of the supernatant was measured at an excitation of 485 nm and an emission of 530 nm on a microplate reader. The ROS contents in the mouse lung tissues were quantified using a DCF standard curve, and the ROS contents were expressed as micromole DCF formed per milligram of protein (μmol DCF formed/mg protein).

Determination of the Pulmonary Vascular Permeability of the Mice

Changes in the pulmonary vascular permeability of the mice were determined using assays through EBD tissue extravasation [21, 22] and the leakage of FITC-albumin

[23] through lungs and blood vessel walls to assess pulmonary vascular permeability.

EBD assay. The mice were administered with EBD (4 mg/kg) through tail vein injection. After 30 min of blood circulation, the mice were intraperitoneally anesthetized with 4% chloral hydrate. After the lungs were perfused with normal saline, approximately 60 mg of lung tissues was weighed. The lung tissues were homogenized after formamide was added and dried in an oven at a constant temperature of 60 °C for 24–48 h, and the supernatant was centrifuged at 12000×*g* for 10 min. The optical density of the supernatant was measured at 620 nm on a microplate reader, and the EBD contents were expressed as nanogram per milligram of lungs (ng per mg lungs).

FITC-albumin assay. The mice were administered with FITC-albumin (20 mg/mL, Abcam) through tail vein injection. After 1 h of blood circulation, the mice were laced under 4% chloral hydrate anesthesia through intraperitoneal injection. The lung tissues perfused with normal saline and 4% formaldehyde dye fixative agent were obtained, fixed for 24 h in 4% paraformaldehyde, and dehydrated for 12 h. The samples were embedded in paraffin, sliced, and dewaxed. After the samples were heated for antigen retrieval, the lung tissues were washed thrice with PBS (5 min/each time), blocked in rabbit serum blocking solution for 30 min at 37 °C, and incubated overnight with thrombomodulin/BDCA-3 antibody (R&D Systems, USA). Then, the samples were washed thrice with PBS (5 min/each time), blocked for 30 min in rabbit serum blocking solution (Zhongshan Golden Bridge Biotechnology, Beijing), and incubated with anti-FITC antibody (Abcam, USA) overnight. The samples were allowed to stand for 30 min at room temperature on the following day. Then, the samples were washed again thrice with PBS (5 min/each time). The rabbit anti-goat fluorescent secondary antibody (Bioss, China) was added dropwise, and the samples were incubated for 1 h at room temperature. After DAPI (Sigma-Aldrich, USA) staining was conducted, the samples were sealed with an anti-fade fluorescence medium (Solarbio, China) and observed under a fluorescent microscope (Olympus, Japan). Afterward, the relative quantitative processing of fluorescence intensity was conducted using Image J software.

Immunofluorescence Techniques

After dewaxing and heating were performed for antigen retrieval, the paraffin sections of the lung tissues were washed thrice with PBS (5 min/each time) and blocked for 1 h in goat serum blocking solution (Zhongshan Golden Bridge Biotechnology, Beijing) at 37 °C. The samples were incubated overnight with SDC-1 or MMP-9 antibody and then allowed to stand for 30 min at room temperature on the following day. They were subsequently washed thrice with PBS (5 min/each time). Goat anti-rabbit IgG/Alexa Fluor 594 antibody was added dropwise, and the samples were incubated for 1 h at room temperature. After DAPI staining was conducted, the samples were sealed with an anti-fade fluorescence medium (Solarbio, China), and the mean fluorescence intensity of SDC-1 or MMP-9 was observed under a fluorescent microscope. The relative quantitative processing of fluorescence intensity was carried out using Image J software.

Determination of the SDC-1 Content in the Serum

The blood samples were collected from the eyeballs of the mice and centrifuged at 4000 rpm for 20 min. The supernatant was collected to determine the SDC-1 content in the serum by using a murine CD138 ELISA kit in accordance with the manufacturer's instructions. Optical density was measured at 450 nm by using a microplate reader, and the SDC-1 contents in the serum were quantified with a CD138 standard curve and expressed as nanogram per milliliter (ng/mL).

Western Blot

Approximately 60–80 mg of mouse lung tissues was weighed and cut into pieces. Then, radioimmunoprecipitation assay (RIPA) buffer (Solarbio, China) and phenylmethylsulfonyl fluoride (Solarbio, China) were added, the samples were homogenized ultrasonically, and the supernatant was collected after centrifugation was performed. The protein concentration was determined with BCA kits (Beyotime Biotechnology, China). Lung-related proteins after SDS-PAGE separation were transferred to PVDF membranes and blocked in 5% skim milk powder at room temperature. After the antibody was added to JNK, ERK, p38, p-JNK, p-ERK, p-p38, NF-κB/p65, IκBα, p-IκBα, β-actin, and Lamin B1 and incubation was performed at 4 °C overnight, the proteins were placed in an oven at a constant temperature of 37 °C for 30 min. The samples were washed thrice with Tris-buffered saline with Tween 20 (TBST, 10 min/each time), and peroxidase-conjugated AffiniPure goat anti-rabbit IgG (Zhongshan Golden Bridge Biotechnology, China) was added. The samples were then incubated for 1 h at room temperature. After the samples were washed with

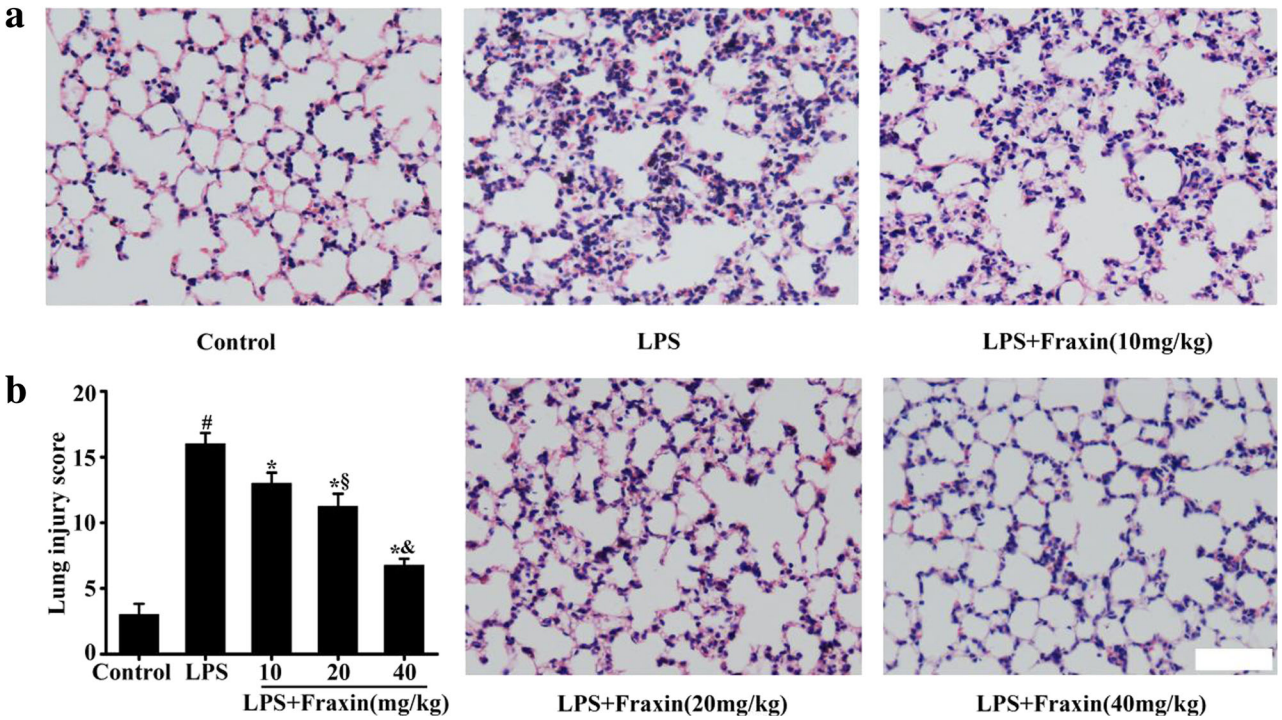

Fig. 1. Effects of fraxin on the pathological changes in the lung tissues of the mice with LPS-induced ARDS. The C57BL/6 mice were intragastrically administered with 10, 20, and 40 mg/kg fraxin for 7 consecutive days and intraperitoneally treated with 20 mg/kg LPS ($n = 6$/group). After 6 h, the lung tissues of the mice were sampled. The pathological changes in the lung tissues of the mice were observed by H&E staining (magnification × 200, scale bar 50 μm) (**a**), and the lung injury score was evaluated (**b**). Data were presented as mean ± SD of three independent experiments. #$p < 0.05$ compared with the control group; *$p < 0.05$ compared with the LPS group; §$p < 0.05$ compared with LPS + fraxin (10 mg/kg) group; &$p < 0.05$ compared with LPS + fraxin (20 mg/kg) group.

TBST, the proteins were stained and exposed with ECL reagents. The gray values of the protein bands were examined with Image J software.

Statistical Analysis

The experiments for each group were repeated thrice. Data were expressed as mean ± standard deviation. Data

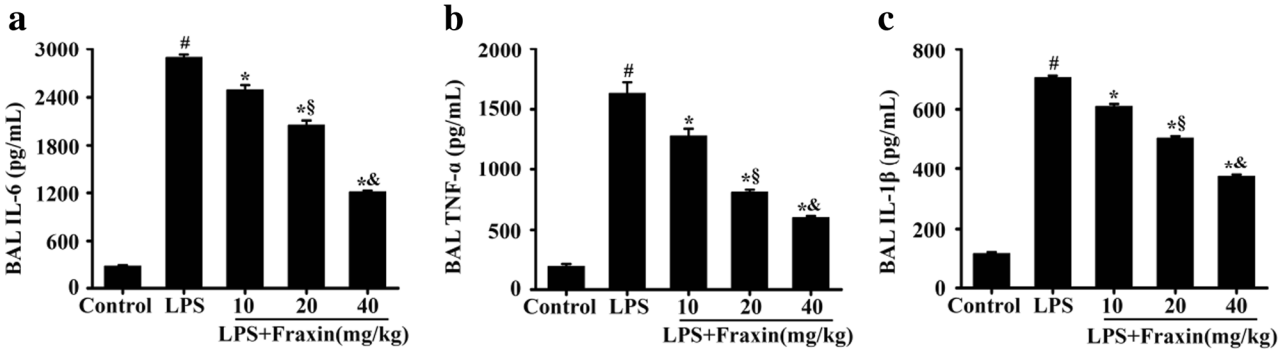

Fig. 2. Effects of fraxin on the IL-6, TNF-α, and IL-1β contents in the BALF of the mice with LPS-induced ARDS. The C57BL/6 mice were intragastrically administered with 10, 20, and 40 mg/kg fraxin for 7 consecutive days and intraperitoneally treated with 20 mg/kg LPS ($n = 6$/group). After 6 h, the BALF was sampled. The contents of the pro-inflammatory cytokines IL-6 (**a**), TNF-α (**b**), and IL-1β (**c**) were detected using commercial ELISA kits. Data were presented as mean ± SD of three independent experiments. #$p < 0.05$ compared with the control group; *$p < 0.05$ compared with the LPS group; §$p < 0.05$ compared with LPS + fraxin (10 mg/kg) group; &$p < 0.05$ compared with LPS + fraxin (20 mg/kg) group.

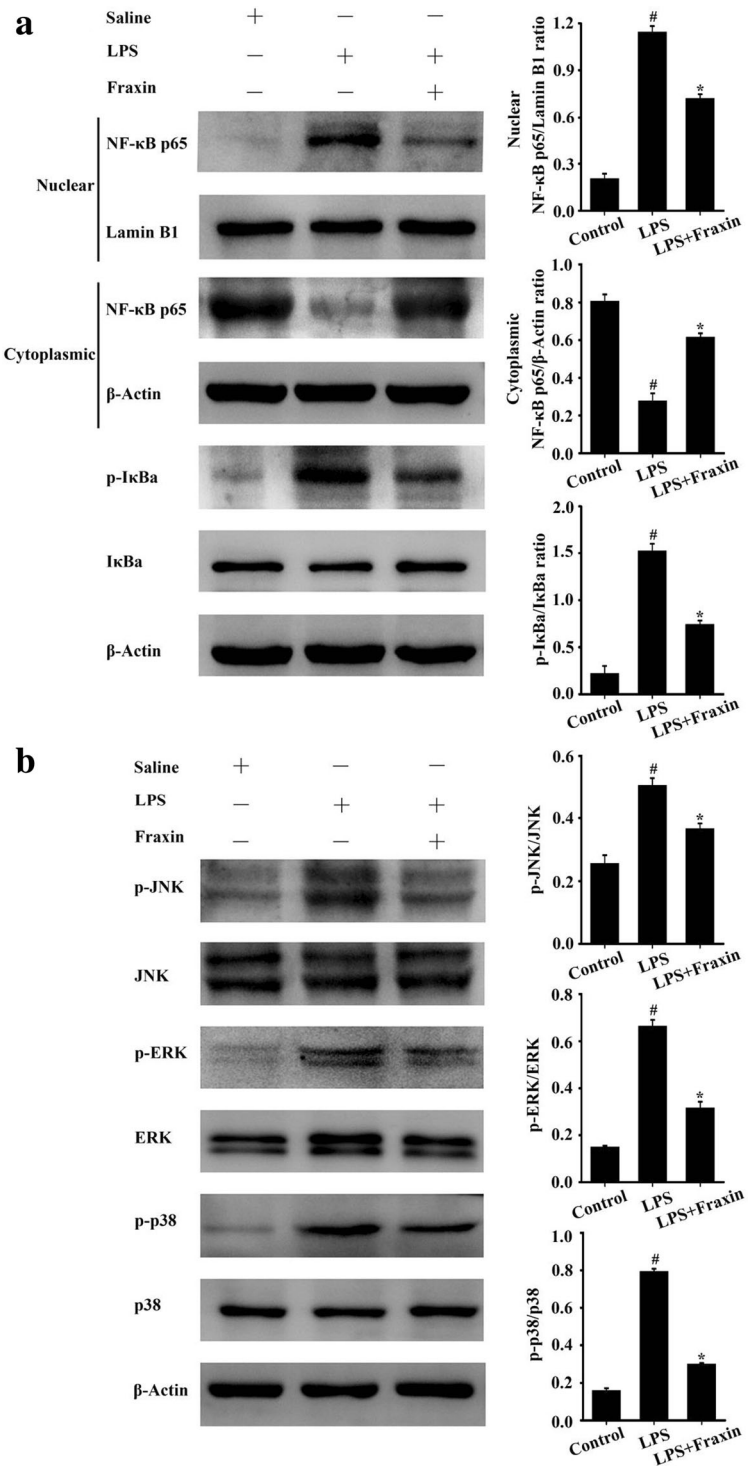

Fig. 3. Effects of fraxin on the NF-κB and MAPK signaling pathways in the lung tissues of the mice with LPS-induced ARDS. The C57BL/6 mice were intragastrically administered with 40 mg/kg fraxin for 7 consecutive days and intraperitoneally treated with 20 mg/kg LPS ($n = 6$/group). The effects of fraxin on the NF-κB (**a**) and MAPK (**b**) signaling pathways in the lung tissues of the mice were assessed with Western blot. Data were presented as mean ± SD of three independent experiments. #$p < 0.05$ compared with the control group; *$p < 0.05$ compared with the LPS group.

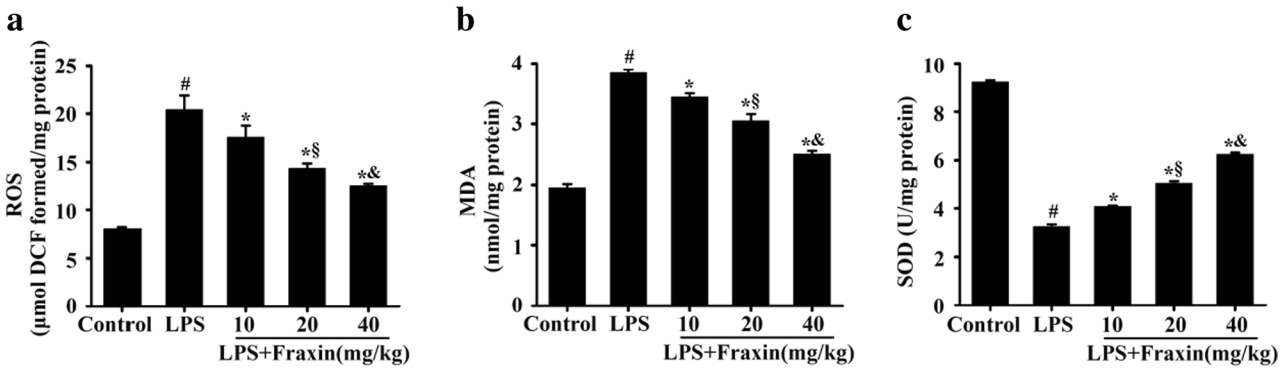

Fig. 4. Effects of fraxin on the ROS and MDA contents and the SOD activity in the lung tissues of the mice with LPS-induced ARDS. The C57BL/6 mice were intragastrically administered with 10, 20, and 40 mg/kg fraxin for 7 consecutive days and intraperitoneally treated with 20 mg/kg LPS ($n = 6$/group). The ROS content (**a**) in the lung tissues of the mice was detected using the fluorescent probe DCFH-DA. The MDA content (**b**) and the SOD activity (**c**) were determined using commercial ELISA kits. Data were presented as mean ± SD of three independent experiments. #$p < 0.05$ compared with the control group; *$p < 0.05$ compared with the LPS group; §$p < 0.05$ compared with LPS + fraxin (10 mg/kg) group; &$p < 0.05$ compared with LPS + fraxin (20 mg/kg) group.

were statistically analyzed using SPSS 17.0. Two groups were compared by Student's *t* test, whereas multiple groups were compared with one-way ANOVA. Pairwise comparison between groups was conducted *via* an SNK test, and statistical significance was determined at $p < 0.05$.

RESULTS

Effects of Fraxin on the Pathological Changes in the Lung Tissues of LPS-Induced ARDS Mice

The lung tissues were observed by H&E staining to assess the effects of fraxin on the pathological changes in the lung tissues of the mice with ARDS. The results showed that fraxin might reduce damages to the alveolar networks, the thickening of the alveolar septa, and the infiltration of inflammatory cells. And the protective effects on the damages to lung tissues became more evident as the concentration of fraxin increased (Fig. 1).

Effects of Fraxin on the IL-6, TNF-α, and IL-1β Contents in the BALF of Mice with LPS-Induced ARDS

Consistent with a previous study [24, 25], our study revealed that the contents of the pro-inflammatory cytokines IL-6, TNF-α, and IL-1β in the BALF of the mice with ARDS increased significantly (Fig. 2a–c), but fraxin treatment reduced the increase in the contents of these pro-inflammatory cytokines. The inhibitory effects on these contents also increased as the fraxin concentration increased (Fig. 2).

Effects of Fraxin on the NF-κB and MAPK Signaling Pathways in the Lung Tissues of the Mice with LPS-Induced ARDS

The effects of fraxin on the activation of the two important inflammatory regulatory pathways, NF-κB and MAPK, were further analyzed through Western blot.

In Fig. 3a, the levels of NF-κB/p65 nuclear translocation and IκBα phosphorylation (p-IκBα) increased significantly in the LPS group compared with those in the control group, indicating the activation of the NF-κB signaling pathway. After fraxin treatment was administered, the levels of NF-κB/p65 nuclear translocation and p-IκBα decreased.

In Fig. 3b, the phosphorylation levels of JNK, ERK, and p38 increased in the LPS group compared with those in the control group, indicating the activation of the MAPK signaling pathway. After fraxin treatment was administered, the p-JNK, p-ERK, and p-p38 levels were significantly inhibited. Therefore, fraxin could effectively inhibit the activation of NF-κB and MAPK signaling pathways.

Effects of Fraxin on Oxidative Damages in the Lung Tissues of Mice with LPS-Induced ARDS

In Fig. 4a and b, the accumulation of ROS and the byproduct of lipid peroxidation MDA content significantly increased in the LPS group. After fraxin treatment was administered, the ROS and MDA contents decreased significantly, indicating that fraxin could significantly reduce

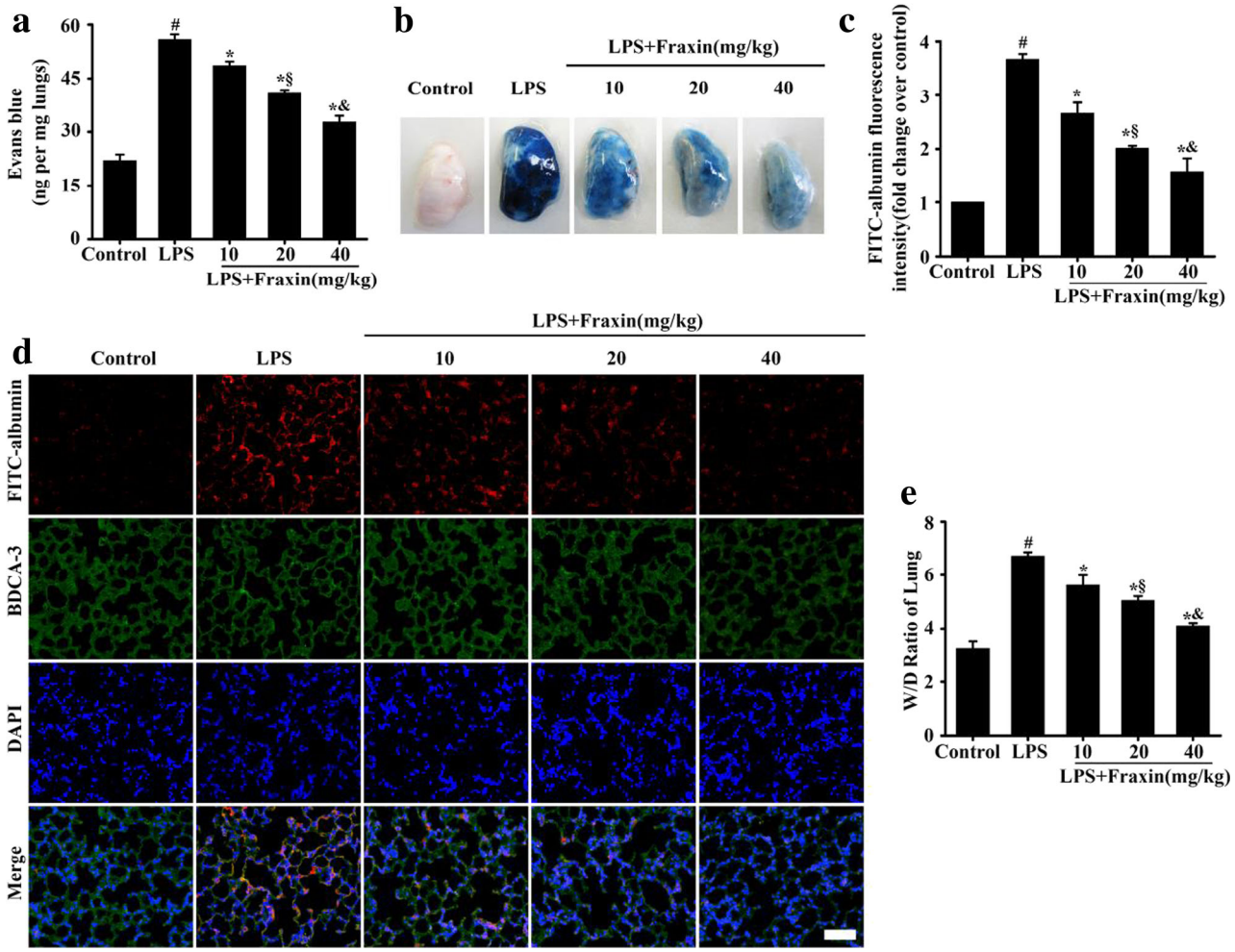

Fig. 5. Effects of fraxin on pulmonary vascular permeability and pulmonary edema in the mice with LPS-induced ARDS. The C57BL/6 mice were intragastrically administered with 10, 20, and 40 mg/kg fraxin for 7 consecutive days and intraperitoneally treated with 20 mg/kg LPS ($n = 6$/group). EBD (**a**, **b**) or FITC-albumin (**c**, **d**) were administered through tail vein injection to detect pulmonary vascular permeability ($n = 6$/group, magnification × 200, scale bar 50 μm). The severity of pulmonary edema in the mice was assessed in terms of the W/D ratio (**e**). Data were presented as mean ± SD of three independent experiments. #$p < 0.05$ compared with the control group; *$p < 0.05$ compared with the LPS group; §$p < 0.05$ compared with LPS + fraxin (10 mg/kg) group; &$p < 0.05$ compared with LPS + fraxin (20 mg/kg) group.

the level of oxidative damage in the lung tissues of the mice with ARDS.

SOD is one of the most important antioxidant enzymes [4]. In Fig. 4c, the SOD activity in the lung tissues of the LPS group significantly decreased, whereas the SOD activity in the lung tissues of fraxin-treated groups substantially increased as the concentration of fraxin increased, and this observation was beneficial to the recovery of the oxidation and antioxidant system balance in the pathogenesis of ARDS.

Effects of Fraxin on Pulmonary Vascular Permeability and Pulmonary Edema in Mice with LPS-Induced ARDS

The effects of fraxin on pulmonary vascular permeability in the mice with ARDS were assessed by measuring EBD and FITC-albumin leakage. The vascular leakage of EBD and FITC-albumin in the ARDS mouse model was significantly inhibited after fraxin treatment was administered, and the inhibitory effects increased as the fraxin concentration increased (Fig. 5a–d).

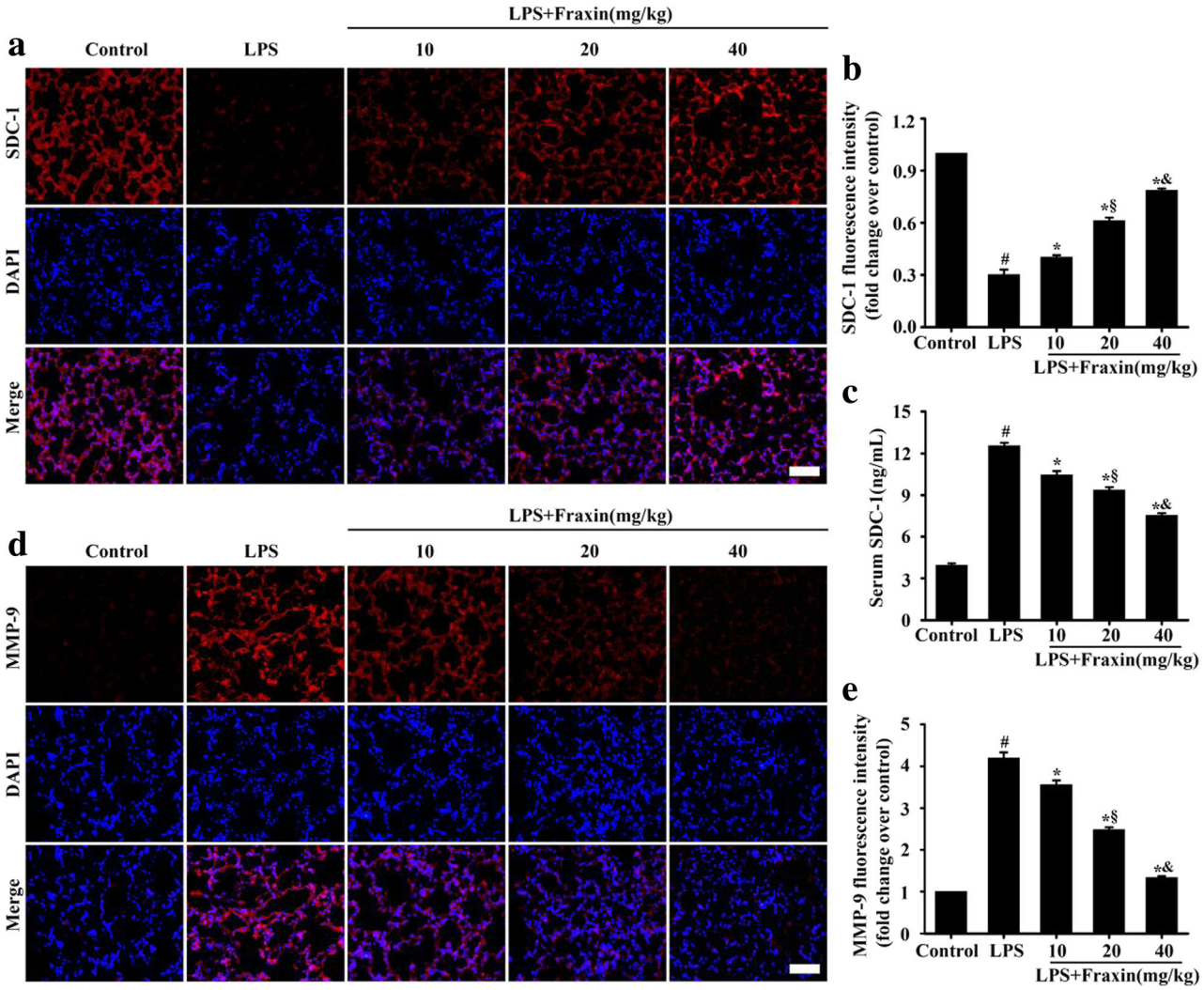

Fig. 6. Effects of fraxin on the integrity of endothelial glycocalyx and the expression of the glycocalyx-degrading enzyme MMP-9 in the mice with LPS-induced ARDS. The C57BL/6 mice were intragastrically administered with 10, 20, and 40 mg/kg fraxin for 7 consecutive days and intraperitoneally treated with 20 mg/kg LPS ($n = 6$/group). After 6 h, the blood and the lung tissues were sampled. The SDC-1 content (**a**; magnification × 200, scale bar 50 μm) and the MMP-9 expression (**d**; magnification × 200, scale bar 50 μm) in the lung tissues of the mice were detected through immunofluorescence techniques. Panels **b** and **e** were the fluorescent quantitation results of **a** and **d**. The serum SDC-1 content (**c**) was detected using commercial ELISA kits. Data were presented as mean ± SD of three independent experiments. #$p < 0.05$ compared with the control group; *$p < 0.05$ compared with the LPS group; §$p < 0.05$ compared with LPS + fraxin (10 mg/kg) group; &$p < 0.05$ compared with LPS + fraxin (20 mg/kg) group.

An increase in pulmonary vascular permeability might trigger pulmonary edema. The severity of lung edema might be assessed by the lung W/D ratio of the lung tissues. The W/D ratio in the mice with ARDS declined sharply after fraxin treatment was administered, indicating that fraxin might alleviate the severity of pulmonary edema in the mice with ARDS, and the severity of pulmonary edema might decrease as the fraxin concentration increased (Fig. 5e).

Effects of Fraxin on the Endothelial Glycocalyx Integrity and the Expression of the Glycocalyx-Degrading Enzyme MMP-9 in Mice with LPS-Induced ARDS

SDC-1 is one of the main components of the endothelial glycocalyx in pulmonary blood vessels, and it is often used to assess damages to the endothelial glycocalyx [4, 26]. Consistent with previous reports, our results showed that the SDC-1

content in the lung tissues was reduced significantly (Fig. 6a and b), and the shedding of the SDC-1 content in serum (Fig. 6c) increased in the mice with ARDS, indicating that the integrity of the endothelial glycocalyx was damaged. Fraxin treatment inhibited the shedding of SDC-1 from the endothelial glycocalyx (Fig. 6a–c), and the protective effects on the shedding of SDC-1 were more evident as the effective concentration of fraxin increased.

Considering that MMP-9 is a SDC-1-specific degrading enzyme [27, 28], the expression level of MMP-9 was further analyzed. In Fig. 6d and e, the MMP-9 level significantly increased in the lung tissues of the mice with ARDS. After fraxin treatment was administered, the increase in MMP-9 was inhibited, and the inhibitory effects became evident as the concentration of fraxin increased.

DISCUSSION

Gram-negative bacterial infection is an important factor leading to ARDS, and LPS is an important virulence factor of these bacteria [29, 30]. In the present study, fraxin exhibited a protective effect on the LPS-induced ARDS mouse model. This effect was manifested by alleviating pathological changes in the lung tissues, reducing the oxidative damages to the lung tissues, decreasing the production of inflammatory factors (IL-6, TNF-α, and IL-1β), activating inflammation-regulatory signaling pathways (NF-κB and MAPK), and downregulating pulmonary vascular permeability (Fig. 7).

The onset and development of ARDS involve large-scale inflammatory responses, and excessive inflammatory responses damage organs or tissues [31]. Therefore, effectively controlling these inflammatory responses is one of the important measures for the treatment of ARDS [5, 32]. In this study, fraxin may significantly inhibit the activation of MAPK and NF-κB signaling pathways in regulating the inflammation and the increase in the concentrations of inflammatory factors (IL-6, TNF-α, and IL-1β) in the LPS-induced ARDS mouse model. This result is consistent with that in previous studies. For example, Niu *et al*. reported that fraxin may significantly inhibit inflammatory responses in a liver injury-induced model by carbon tetrachloride induced in

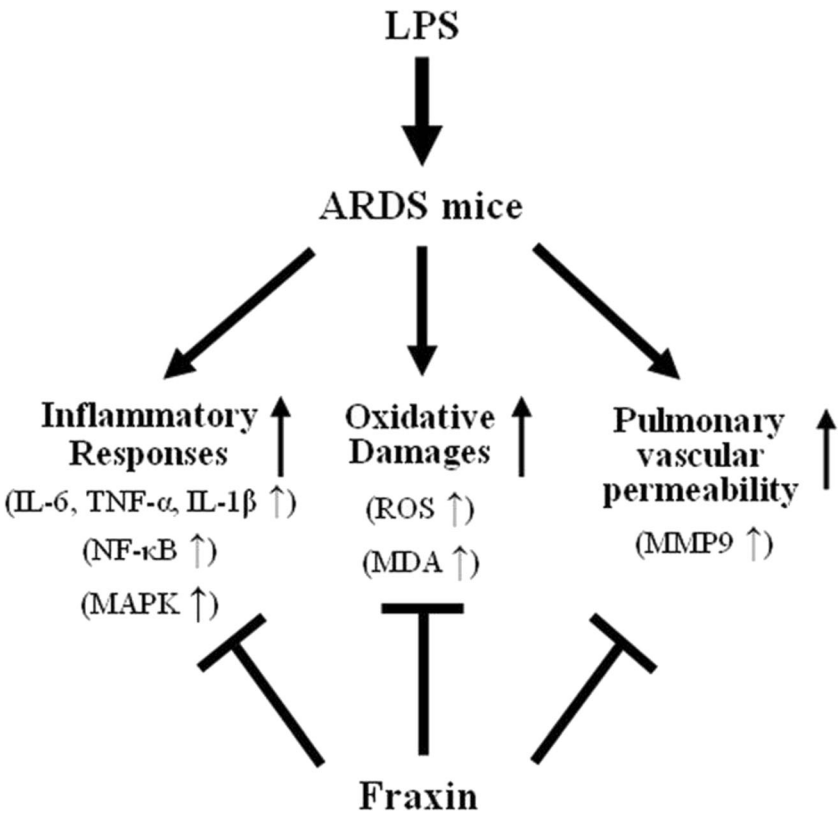

Fig. 7. Scheme summarizing the protective effects of fraxin on mice with LPS-induced ARDS. Fraxin alleviated LPS-induced ARDS by downregulating inflammatory responses and oxidative damages and reducing pulmonary vascular permeability.

mice and the activation of the MAPK signaling pathway [13]. These experimental results indicated that fraxin may play an enhanced anti-inflammation role in inflammatory responses induced by different factors.

Oxidative damages are another important factors for tissue cell damages in the pathogenesis of ARDS [33, 34]. In the present study, fraxin effectively reduced the levels of oxidative damage and promoted the recovery of oxidation/antioxidant balance in the lung tissues of the mice with LPS-induced ARDS. The effective inhibition of inflammatory responses is another important mechanism of action of fraxin on ARDS.

Increased vascular permeability is one of the important pathological features of ARDS [35, 36]. This study found that fraxin treatment could reduce the increase in vascular permeability in the lung tissue of the mice with LPS-induced ARDS. The endothelial glycocalyx, which is an important barrier to maintain vascular permeability, was destroyed during the onset of ARDS [8, 9]. Furthermore, fraxin treatment could inhibit the expression of MMP-9 and reduce the destruction of endothelial glycocalyx (SDC-1 shedding), indicating that fraxin inhibited the increase in vascular permeability at least partially by maintaining the integrity of endothelial glycocalyx.

In conclusion, fraxin attenuated LPS-induced ARDS by downregulating inflammatory responses and oxidative damage and reducing pulmonary vascular permeability.

FUNDING INFORMATION

This work was supported by funding from the Natural Science Foundation of Shandong Province, China (ZR2017MH065), Young Teachers' Training and Funding Project of Binzhou Medical University, and the National Natural Science Foundation of China (No. 81670078).

COMPLIANCE WITH ETHICAL STANDARDS

Conflict of Interest. The authors declare that they have no conflict of interest.

REFERENCES

1. Laffey, J.G., and B.P. Kavanagh. 2017. Fifty years of research in ARDS. Insight into acute respiratory distress syndrome. From models to patients. *American Journal of Respiratory and Critical Care Medicine* 196 (1): 18–28.
2. Ferguson, N.D., E. Fan, L. Camporota, M. Antonelli, A. Anzueto, R. Beale, L. Brochard, R. Brower, A. Esteban, L. Gattinoni, A. Rhodes, A.S. Slutsky, J.L. Vincent, G.D. Rubenfeld, B.T. Thompson, and V.M. Ranieri. 2012. The Berlin definition of ARDS: an expanded rationale, justification, and supplementary material. *Intensive Care Medicine* 38 (10): 1573–1582.
3. Máca, J., O. Jor, M. Holub, P. Sklienka, F. Burša, M. Burda, V. Janout, and P. Ševčík. 2017. Past and present ARDS mortality rates: a systematic review. *Respiratory Care* 62 (1): 113–122.
4. Liu, X.Y., H.X. Xu, J.K. Li, D. Zhang, X.H. Ma, L.N. Huang, J.H. Lü, and X.Z. Wang. 2018. Neferine protects endothelial glycocalyx via mitochondrial ROS in lipopolysaccharide-induced acute respiratory distress syndrome. *Frontiers in Physiology* 9: 102.
5. Kong, G., X. Huang, L. Wang, Y. Li, T. Sun, S. Han, W. Zhu, M. Ma, H. Xu, J. Li, X. Zhang, X. Liu, and X. Wang. 2016. Astilbin alleviates LPS-induced ARDS by suppressing MAPK signaling pathway and protecting pulmonary endothelial glycocalyx. *International Immunopharmacology* 36: 51–58.
6. Hsu, H.T., Y.T. Tseng, Y.Y. Hsu, K.I. Cheng, S.H. Chou, and Y.C. Lo. 2015. Propofol attenuates lipopolysaccharide-induced reactive oxygen species production through activation of Nrf2/GSH and suppression of NADPH oxidase in human alveolar epithelial cells. *Inflammation* 38 (1): 415–423.
7. Lei, J., Y. Wei, P. Song, Y. Li, T. Zhang, Q. Feng, and G. Xu. 2018. Cordycepin inhibits LPS-induced acute lung injury by inhibiting inflammation and oxidative stress. *European Journal of Pharmacology* 818: 110–114.
8. Yang, Y., and E.P. Schmidt. 2013. The endothelial glycocalyx: an important regulator of the pulmonary vascular barrier. *Tissue Barriers* 1 (1): 23494.
9. Inagawa, R., H. Okada, G. Takemura, K. Suzuki, C. Takada, H. Yano, Y. Ando, T. Usui, Y. Hotta, N. Miyazaki, A. Tsujimoto, R. Zaikokuji, A. Matsumoto, T. Kawaguchi, T. Doi, T. Yoshida, S. Yoshida, K. Kumada, H. Ushikoshi, I. Toyoda, and S. Ogura. 2018. Ultrastructural alteration of pulmonary capillary endothelial glycocalyx during endotoxemia. *Chest* 154 (2): 317–325.
10. Kostova, I. 2001. Fraxinus ornus L. *Fitoterapia* 72 (5): 471–480.
11. Wang, H., B. Xiao, Z. Hao, and Z. Sun. 2016. Simultaneous determination of fraxin and its metabolite, fraxetin, in rat plasma by liquid chromatography-tandem mass spectrometry and its application in a pharmacokinetic study. *Journal of Chromatography B: Analytical Technologies in the Biomedical and Life Sciences* 1017-1018: 70–74.
12. Chang, B.Y., Y.S. Jung, C.S. Yoon, J.S. Oh, J.H. Hong, Y.C. Kim, and S.Y. Kim. 2017. Fraxin prevents chemically induced hepatotoxicity by reducing oxidative stress. *Molecules* 22 (4): E587.
13. Niu, X., F. Liu, W. Li, W. Zhi, Q. Yao, J. Zhao, G. Yang, X. Wang, L. Qin, and Z. He. 2017. Hepatoprotective effect of fraxin against carbon tetrachloride-induced hepatotoxicity in vitro and in vivo through regulating hepatic antioxidant, inflammation response and the MAPK-NF-κB signaling pathway. *Biomedicine & Pharmacotherapy* 95: 1091–1102.
14. Whang, W.K., H.S. Park, I. Ham, M. Oh, H. Namkoong, H.K. Kim, D.W. Hwang, S.Y. Hur, T.E. Kim, Y.G. Park, J.R. Kim, and J.W. Kim. 2005. Natural compounds, fraxin and chemicals structurally related to fraxin protect cells from oxidative stress. *Experimental and Molecular Medicine* 37 (5): 436–446.
15. Schempp, H., D. Weiser, and E.F. Elstner. 2000. Biochemical model reactions indicative of inflammatory processes. Activities of extracts from Fraxinus excelsior and Populus tremula. *Arzneimittel-Forschung/Drug Research* 50 (4): 362–372.

16. Song, L., Z. Han, H. Cheng, J. Huan, L. Chen, J. Meng, X. Chen, and L. Xie. 2018. Therapeutic effects of different doses of methylprednisolone on smoke inhalation-induced acute lung injury in rats. *Zhongguo Wei Zhong Bing Ji Jiu Yi Xue* 30 (8): 754–759.
17. Wang, L., X. Huang, G. Kong, H. Xu, J. Li, D. Hao, T. Wang, S. Han, C. Han, Y. Sun, X. Liu, and X. Wang. 2016. Ulinastatin attenuates pulmonary endothelial glycocalyx damage and inhibits endothelial heparanase activity in LPS-induced ARDS. *Biochemical and Biophysical Research Communications* 478 (2): 669–675.
18. Wang, C., L. Zeng, T. Zhang, J. Liu, and W. Wang. 2016. Casticin inhibits lipopolysaccharide-induced acute lung injury in mice. *European Journal of Pharmacology* 789: 172–178.
19. Zhang, Z., Z. Luo, A. Bi, W. Yang, W. An, X. Dong, R. Chen, S. Yang, H. Tang, X. Han, and L. Luo. 2017. Compound edaravone alleviates lipopolysaccharide (LPS)-induced acute lung injury in mice. *European Journal of Pharmacology* 811: 1–11.
20. Lincoln, K.M., P. Gonzalez, T.E. Richardson, D.A. Julovich, R. Saunders, J.W. Simpkins, and K.N. Green. 2013. A potent antioxidant small molecule aimed at targeting metal-based oxidative stress in neurodegenerative disorders. *Chemical Communications* 49 (26): 2712–2714.
21. Beatty, P.R., H. Puerta-Guardo, S.S. Killingbeck, D.R. Glasner, K. Hopkins, and E. Harris. 2015. Dengue virus NS1 triggers endothelial permeability and vascular leak that is prevented by NS1 vaccination. *Science Translational Medicine* 7 (304): 304ra141.
22. Aimbire, F., A.P. Ligeiro de Oliveira, R. Albertini, J.C. Corrêa, C.B. Ladeira de Campos, J.P. Lyon, J.A.Jr. Silva, and M.S. Costa. 2008. Low level laser therapy (LLLT) decreases pulmonary microvascular leakage, neutrophil influx and IL-1beta levels in airway and lung from rat subjected to LPS-induced inflammation. *Inflammation* 31 (3): 189–197.
23. Esiobu, P., and E.W. Childs. 2018. A rat model of hemorrhagic shock for studying vascular hyperpermeability. *Methods in Molecular Biology* 1717: 53–60.
24. Bhargava, R., W. Janssen, C. Altmann, A. Andrés-Hernando, K. Okamura, R.W. Vandivier, N. Ahuja, and S. Faubel. 2013. Intratracheal IL-6 protects against lung inflammation in direct, but not indirect, causes of acute lung injury in mice. *PLoS One* 8 (5): e61405.
25. Ju, Y.N., J. Gong, X.T. Wang, J.L. Zhu, and W. Gao. 2018. Endothelial colony-forming cells attenuate ventilator-induced lung injury in rats with acute respiratory distress syndrome. *Archives of Medical Research* 49 (3): 172–181.
26. Peng, Z., S. Pati, D. Potter, R. Brown, J.B. Holcomb, R. Grill, K. Wataha, P.W. Park, H. Xue, and R.A. Kozar. 2013. Fresh frozen plasma lessens pulmonary endothelial inflammation and hyperpermeability after hemorrhagic shock and is associated with loss of syndecan 1. *Shock* 40 (3): 195–202.
27. Szatmári, T., R. Ötvös, A. Hjerpe, and K. Dobra. 2015. Syndecan-1 in cancer: implications for cell signaling, differentiation, and prognostication. *Disease Markers* 2015: 796052.
28. Wang, X., D. Zuo, Y. Chen, W. Li, R. Liu, Y. He, L. Ren, L. Zhou, T. Deng, X. Wang, G. Ying, and Y. Ba. 2014. Shed Syndecan-1 is involved in chemotherapy resistance via the EGFR pathway in colorectal cancer. *British Journal of Cancer* 111 (10): 1965–1976.
29. Qi, D., X. Tang, J. He, D. Wang, Y. Zhao, W. Deng, X. Deng, G. Zhou, J. Xia, X. Zhong, and S. Pu. 2016. Omentin protects against LPS-induced ARDS through suppressing pulmonary inflammation and promoting endothelial barrier via an Akt/eNOS-dependent mechanism. *Cell Death & Disease* 7 (9): e2360.
30. Xiao, M., T. Zhu, W. Zhang, T. Wang, Y.C. Shen, Q.F. Wan, and F.Q. Wen. 2014. Emodin ameliorates LPS-induced acute lung injury, involving the inactivation of NF-κB in mice. *International Journal of Molecular Sciences* 15 (11): 19355–19368.
31. Ma, M.M., Y. Li, X.Y. Liu, W.W. Zhu, X. Ren, G.Q. Kong, X. Huang, L.P. Wang, L.Q. Luo, and X.Z. Wang. 2015. Cyanidin-3-O-glucoside ameliorates lipopolysaccharide-induced injury both in vivo and in vitro suppression of NF-κB and MAPK pathways. *Inflammation* 38 (4): 1669–1682.
32. Zhou, F., Y. Zhang, J. Chen, X. Hu, and Y. Xu. 2016. Liraglutide attenuates lipopolysaccharide-induced acute lung injury in mice. *European Journal of Pharmacology* 791: 735–740.
33. Chen, L., W. Li, D. Qi, L. Lu, Z. Zhang, and D. Wang. 2018. Honokiol protects pulmonary microvascular endothelial barrier against lipopolysaccharide-induced ARDS partially via the Sirt3/AMPK signaling axis. *Life Sciences* 210: 86–95.
34. Chen, L., W. Li, D. Qi, and D. Wang. 2018. Lycium barbarum polysaccharide protects against LPS-induced ARDS by inhibiting apoptosis, oxidative stress, and inflammation in pulmonary endothelial cells. *Free Radical Research* 52 (4): 480–490.
35. Mammoto, A., T. Mammoto, M. Kanapathipillai, C. Wing Yung, E. Jiang, A. Jiang, K. Lofgren, E.P. Gee, and D.E. Ingber. 2013. Control of lung vascular permeability and endotoxin-induced pulmonary oedema by changes in extracellular matrix mechanics. *Nature Communications* 4: 1759.
36. Perel, A. 2013. Extravascular lung water and the pulmonary vascular permeability index may improve the definition of ARDS. *Critical Care* 17 (1): 108.